Islanding Detection Using Rate of Change of Zero Sequence of Second Harmonic Voltage

Mustafa Mahmoud Abdel-Aziz * ‡, Mahmoud Ibrahim Gilany**, Doaa Khalil Ibrahim***, Aboul Fotouh Abdel-Rheem****

*Department of Electrical Power & Machines Engineering, Higher Institute of Engineering at El-Shorouk City, Cairo, Egypt

**Department of Electrical Power Engineering, Faculty of Engineering, Cairo University, Giza, Egypt

***Department of Electrical Power Engineering, Faculty of Engineering, Cairo University, Giza, Egypt

*****Department of Electrical Power & Machines Engineering, Higher Institute of Engineering at El-Shorouk City, Cairo, Egypt

(mustafa_saadaawy@yahoo.com , drgilany@gmail.com , doaakhalil73@gmail.com and a.abdelreheem@sha.edu.eg)

‡ Corresponding Author; Mustafa Mahmoud Abdel-Aziz, Higher Institute of Engineering at El-Shorouk City , Cairo, Egypt, Tel: +20201019202525, mustafa_saadaawy@yahoo.com.

Received: 07.08.2020 Accepted: 11.09.2020

Abstract- Integration of Distributed Generation (DG) on the power system networks causes several difficulties, especially for the system protection. One of the important problems associated with system protection is the islanding that takes place when a DG unit (or group of units) continues to energize a part of the load separated from the main utility. As a result, many obstacles occur such as voltage and frequency fluctuation, in addition to personnel safety problems during maintenance. In this paper, the islanding problem is discussed and also the previous islanding detection techniques are investigated to get an efficient technique for islanding detection. The proposed technique is based on estimating the Rate of Change of Zero Sequence of Second Harmonic Voltage at the Point of Common Coupling (PCC). The proposed technique is extensively tested for inverter-based DG includes wind turbines with double-fed induction generator (DFIG). The proposed technique could distinguish the islanding operation correctly within only one cycle without non-detection zone (NDZ). In addition, it could differentiate between the islanding operation at different values for active and reactive power mismatch. Several scenarios are tested such as normal load variation, capacitor switching and power quality disturbances like voltage sags and swells. Faults and outage of one of DGs are also tested.

Keywords: Distributed Generation, Islanding Detection, Non-detection Zone, Passive Islanding Detection Techniques, Rate of Change, Second Harmonic.

Nomenclature

DFIG	:	Double Fed Induction Generator
DFT	:	Discrete Fourier Transform
DG	:	Distributed generation
NDZ	:	Non Detection Zone
OV	:	Over Voltage
PCC	:	Point of Common Coupling
$ROCO2Z$	:	Rate of change of zero sequence component of 2nd harmonic voltage
$ROCOF$	:	Rate of Change of Frequency
$ROCOQ$	:	Rate of Change of Reactive Power
$ROCOV$	:	Rate of Change of Voltage
THD	:	Total Harmonic Distortion
UV	:	Under Voltage
F1 and F2	:	Fault Location 1 and 2
V_a, V_b and V_c	:	Three phase voltages measured at PCC
V_{a2}, V_{b2} and V_{c2}	:	Three phase 2nd harmonic voltage at PCC
$V_{2h_z(n)}$	:	RMS value of zero sequence of 2nd harmonic voltage at sample (n)
ΔT	:	Sampling interval

1. Introduction

Huge efforts are made to encourage the expansion of sustainable energy resources, such as wind turbines and photovoltaic systems in the medium voltage distribution systems. Such generation units are called Distributed Generation units (DGs) [1-2]. In general, DGs technologies have good overall efficiencies. Besides, renewable energy based DG units contribute in reducing greenhouse gases. DGs are connected in distribution systems close to load centers to provide many benefits to the customers, utilities and environment [1-2]. But on the other hand, negative impacts occur especially on the distribution system's protection scheme due to the fact that the integration of DGs in distribution systems will deteriorate the radial nature of these systems. In addition, there will be an increasing in the short circuit levels of the network [3], miss-coordination between the protective devices [4], false tripping of the protective devices [5], protection system blinding and islanding.

As a brief explanation for islanding phenomenon; by the grid outage, a part of load is still fed through DGs. Islanding can be classified into intentional and unintentional islanding. Intentional islanding occurs when the DG unit works as a backup to network outage to increase the reliability like UPS. But unintentional islanding is a situation of feeding a part of load through DG or group of DGs, while outage of network occurs [6].

At the present, islanding detection techniques can be categorized into two major groups which are basically remote and local techniques [7]. The remote techniques are based on the communication between utilities and DGs, so they have higher reliability than local detection techniques, but they are expensive to be implemented in distribution systems [8]. The latter methods are divided into active and passive methods. Such local detection techniques are based on measuring some output parameters like voltage, current, or frequency of the DG side to decide if these parameters describe an islanding situation or not [9-10].

Active methods are based on injecting small perturbations in power system, which introduce disturbance in the system unlike passive techniques. Active techniques have many forms such as active frequency drift, Sandia frequency shift that is based on frequency variation to detect islanding operation and pulse current injection. Active techniques detect islanding even under perfect balance between generation and load [11-13]. These techniques depend on injecting a distorted current waveform into the original reference current of the inverter; therefore, in the case of islanding operation the frequency changes up or down. Active techniques occasionally have a bad effect on the system such as voltage fluctuation as discussed in [14].

Passive detection techniques are fast and do not introduce disturbance in the system, but they have a blind area for detecting the islanding operation at zero power mismatch (which is called NDZ) that presents the interval in which islanding detection scheme fails to detect islanding condition. Passive techniques have many forms of monitored quantities depending on the voltage and frequency variation such as under/over voltage and under/over frequency, but these methods have a large non detection zone in case of zero power mismatches [15]. Some other methods depend on the rate of change such as rate of impedance change, rate of frequency change of (ROCOF) [16], rate of change of reactive power (ROCOQ) and voltage (ROCOV) [17]. For example: ROCOF relay calculates the system frequency from measured DG signal which is filtered to remove any noise before finding the rate of change of frequency. Although it has the smallest NDZ, it has high possibility of false tripping [16]. Integrating more of one quantities is also investigated to get a more efficient islanding detection scheme as in [18, 19], where the total harmonic distortion (THD) of current is used jointly with the rate of change of reactive power (ROCOQ) in [18], and with the voltage unbalance in [19]. Also, THD method is compared with impedance estimation method for islanding detection in [20]. Islanding has also been detected in [21] using the second harmonic voltage and current signals in two cycles using artificial neural networks with small NDZ when the power is outside the preset power range.

Generally, number of active and passive islanding detection techniques has used the harmonics as features for islanding detection; the majority of them are passive techniques. In [22], cumulative reactive power harmonics are used to detect the islanding operation within two cycles from its occurrence. Such method can detect islanding without any NDZ, where it was tested for inverter-based DG with different case studies; load change, capacitor switching and islanding scenarios. The variation of the 5th harmonic order is also used as a passive islanding detection method in [23], where islanding situation is detected at microgrid terminal, connected with RLC load after the grid outage by 2 sec without NDZ. The 5th order is also used for islanding detection in [24] with the 3rd and 7th order of harmonics, where the selected harmonic distortion is calculated in each cycle to decide if the operation is islanding or not. This method succeeds to detect islanding from one to two cycles with negligible NDZ. A passive islanding detection method depends on under voltage (UV) and over voltage (OV) with aid of total harmonic distortion (THD) was also proposed in [25]. It was applied at DG terminal for different power mismatch scenarios and islanding situations with minimum NDZ less than the UV and OV methods. Also UV/OV and Under/Over frequency methods are integrated with Sandia frequency shift and sandia voltage shift as a hybrid islanding detection technique as in [13].

As the major weakness points of most of passive detection techniques are the presence of NDZ and large time for islanding detection, the proposed method in this paper aims to overcome these challenges. Accordingly, the proposed method is designated to achieve the following objectives:

- Islanding detection within the standard time of IEEE STD 1547-2003 4.4.1, where the DG should disconnect itself from the network within two seconds from islanding occurrence [26].
- Minimizing the non-detection zone (NDZ).

The organization of this paper is as follows, the second section introduces the suitable order of harmonics used for islanding detection in the proposed method, where the methodology for the proposed islanding detection method is discussed in the third section. Fourth section shows the simulated tested network model. Fifth section demonstrates in details the achieved results and tested events. Finally, the conclusions are drawn in the sixth part.

2. Selecting an Appropriate Order of Harmonic for Islanding Detection

The target of the proposed method is to get benefit from the harmonic content of the voltage signal at PCC. In fact, different orders of harmonics are used in several reported schemes in literature according to the harmonic order that has the largest magnitude in the tested system for each scheme. For example, the 5th harmonic order deviation is applied in the passive islanding detection technique in [23], the 2nd harmonic order of both voltage and current signals are used for islanding discrimination in [21], while the odd 3rd, 5th and 7th harmonic orders are used for identifying the islanding situation in [24]. Actually, all these orders of harmonics are applied as they have the largest magnitude in tested systems, where many factors affect them such as the design of inverter connected to the DG, the type of DG, converter type, the gear box existence beside the nominal voltage and current [27]. Two types of wind turbines are studied in [28] to determine the harmonic orders exist, and it is found that the 2nd harmonic is the largest magnitude in one wind turbine type, while the 5th harmonic has the largest magnitude in the other type.

For the studied system in this paper, according to the existence of DG based-inverter technology, the 2nd harmonic is found to have the maximum contribution compared with other harmonics during the islanding operation as discussed in [21]. Besides, the frequency spectrum during the islanding operation has been studied using MATLAB/Simulink as illustrated in Fig. 1. As obviously shown, the 2nd harmonic is observed to have the maximum contribution, which is also fully matched with [21].

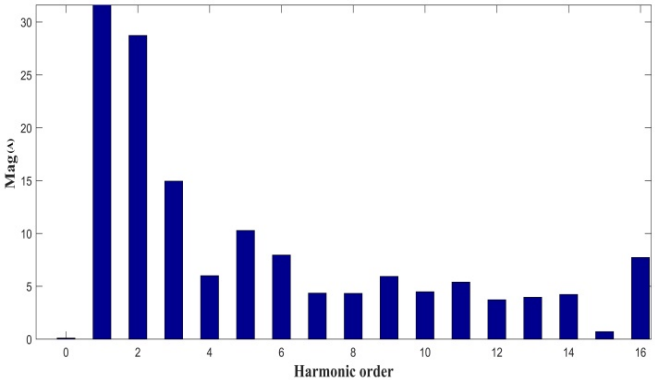

Fig. 1. Magnitude of different harmonics at PCC during islanding operation.

3. Methodology of the Proposed Islanding Detector

Noticing that the second harmonic is the clearest order of harmonic for the tested system due to the existence of inverter and transformer at the DG end, an islanding detection technique is examined through monitoring the rate of change the second harmonic voltage sequences. Fig. 2, evaluates the variation of the rates of change of positive, negative and zero sequence of second harmonic voltage at PCC for three different operating conditions.

- The first condition is the switching event of 2.8 MVAR capacitor at 0.4 sec,
- The second condition is the load switching of 6 MW & 3 MVAR at 0.6 sec,
- The third condition is the islanding condition which is simulated at 0.8 sec.

It is clear from Fig. 2, that the rate of change of zero sequence of second harmonic voltage ($ROCO2Z$) is the best indicator among the three calculated sequences that is not affected by capacitor switching or load switching. Besides, it has a significant variation for islanding condition. Thus $ROCO2Z$ is applied in this paper as a proposed islanding detection index.

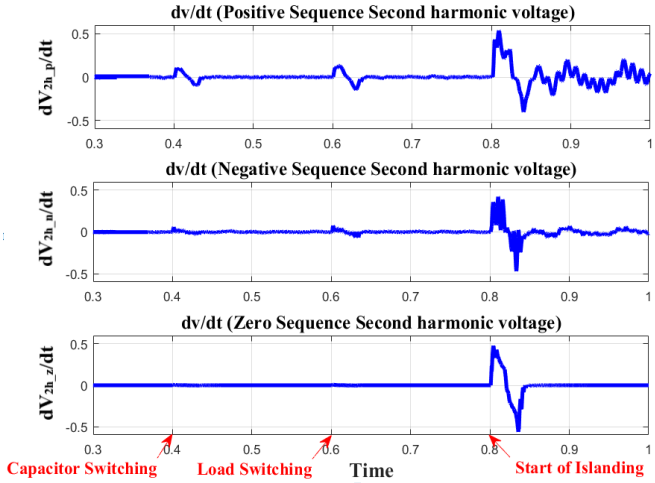

Fig. 2. Rates of change of positive, negative and zero sequence of second harmonic voltage (volt/sec) for different operating conditions.

To implement the proposed islanding detection technique, the following steps are followed:

- The samples of the local measured voltage signals (V_a, V_b and V_c) of the DG output are measured at PCC.
- Full cycle Discrete Fourier Transform (DFT) is applied to extract the second harmonic voltage signals (V_{a2}, V_{b2} and V_{c2}).
- The second harmonic voltage signals V_{a2}, V_{b2} and V_{c2} are directly converted using symmetrical components to get the zero sequence component of the second harmonic voltage (V_{2h_z}) as shown in equation (1):

$$V_{2h_z} = \frac{1}{3}(V_{a2} + V_{b2} + V_{c2}) \quad (1)$$

- After getting the zero sequence components of second harmonic voltage, its rate of change is calculated using equation (2):

$$ROCO2Z = \frac{V_{2h_z(n)} - V_{2h_z(n-1)}}{\Delta T} \quad (2)$$

Where: $V_{2h_z(n)}$ and $V_{2h_z(n-1)}$ are the calculated RMS values of zero sequence of the second harmonic voltage at present sample (n) and previous one $(n-1)$, respectively, while ΔT is the sampling interval.

- Finally, the value of the proposed index $ROCO2Z$ is compared against the threshold value to decide if the event is islanding or not.

Actually, the threshold value for islanding detection for a tested network can be settled by carrying out extensive simulation tests for different scenarios with several sizes of DG at different locations. All scenarios are investigated at the worst case of islanding detection, where the DG size is equal to the connected load.

The proposed islanding detection technique flowchart is demonstrated in Fig. 3.

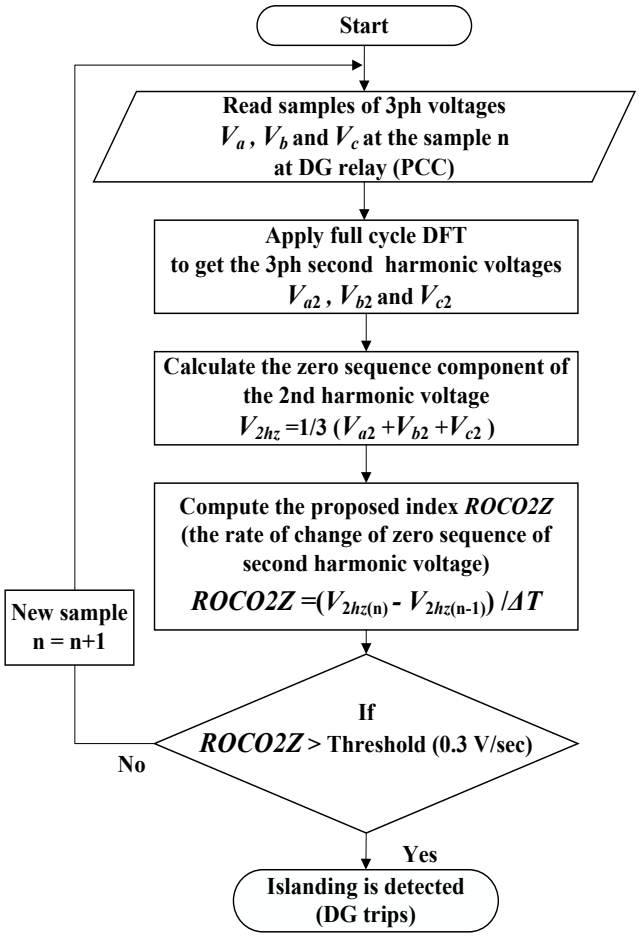

Fig. 3. The flowchart of the proposed technique steps.

4. Modeling of Tested Network

Fig. 4, shows the single line diagram of the 25 kV tested distribution system at 60 Hz frequency. The detailed system parameters can be found in [21] and shown in Table 1. It has one DG unit of 9 MW connected to the Bus 5 that comprises six wind turbines with DFIGs, where each one of them equal 1.5 MW. The network is connected to a 25 kV distribution system at PCC to feed the RLC loads with the main grid. For this tested distribution network and upon carrying out different tests of islanding detection with different sizes of DG at different buses, the threshold value is determined as 0.3 volt/sec.

A second DG is also needed for investigating the last case study of multi DGs as will be shown. This second DG was added at Bus 3 with the same parameters of the main DG. Due to the islanding condition is simulated after one of DG outage, the total generation power by the other DG that remains to feed load is equal to the total load (zero power mismatch). So the threshold value is the same in this case study as only one DG exists during the islanding occurrence. The whole system is simulated and tested using MATLAB/Simulink program.

Table 1. The main parameters of the tested system.

System Parameters	System Data
Grid	2500 MVA, 120 kV, 60 Hz
Grid Transformer T3	Step down: 120 kV/25 kV, 47 MVA, 0.08 pu
Main DG at DG Bus 1, Second DG at DG Bus 2	At 575 V, with Six wind turbines, each has DFIG of 1.5 MW
DG Transformer T1 & T2	Step up: 575 V/25 kV, 10.5 MVA, 0.025 pu
Transmission Lines Parameters: Positive and Zero Sequence R, L and C	R1=0.1153 Ω/km; R0=0.413 Ω/km; X1=1.05 mH/km; X0=3.32 mH/km; C1=11.33 nF/km; C0=5.01 nF/km
Transmission Lines Lengths	20 km for Line 1 10 km for Line 2 & Line 3
Load 1 at Bus 6	Fixed load at 9 MW active power and 4.359 MVAR reactive power
Load 2 at Bus 6	Variable load between 4 MW to 9 MW active power and 2 MVAR to 4.359 MVAR reactive power
Shunt capacitance at Bus 6	1.41 MVAR

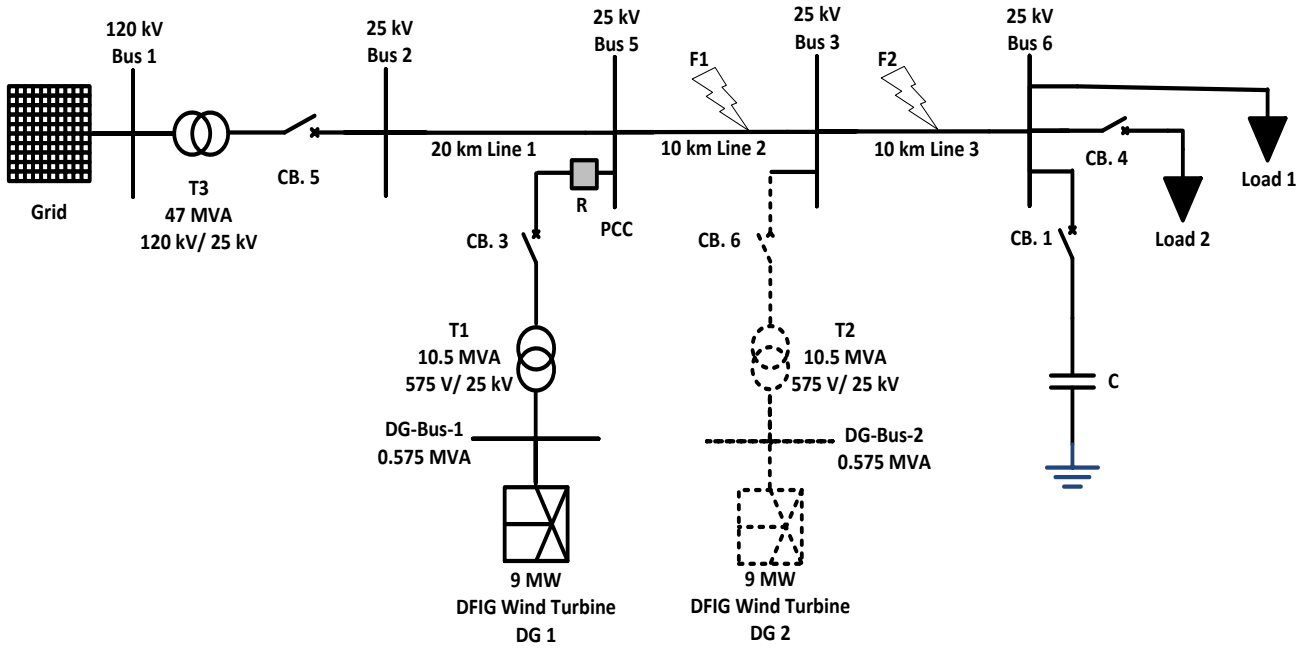

Fig. 4. The single line diagram of the tested network.

5. Simulation Results

The robustness of the proposed islanding detection method is not only its ability to detect the islanding operation within one cycle without non-detection zone, but also its stability during other normal operating conditions. Therefore, the tested simulated cases could be categorized as follows; islanding cases at different values for active and reactive power mismatch (high, low and zero power mismatch), normal switching such as load and capacitor switching, power quality disturbances such as voltage sag and swell, unbalance load, faults and outage of one of DGs. All these conditions are tested in the next subsections.

5.1. Performance of the proposed scheme during different values of active and reactive power mismatch

Table 2 shows the different scenarios for normal operation with different power mismatch besides the islanding operation to evaluate the proposed technique. Where the first scenario presents the large power mismatch, the second scenario presents small power mismatch and finally the third scenario presents zero power mismatch.

Fig. 5, 6 and 7, show the achieved results for the first, the second and the third scenarios respectively, where each figure shows how $ROCO2Z$ differs for normal operation and islanding situation. The grid circuit breaker (CB5 in Fig. 4) is opened at 0.8 sec to create an islanding situation. As shown, $ROCO2Z$ goes above the threshold value in less than half a cycle between 0.802 and 0.805 sec.

The rest of tested case studies will be compared against islanding operation at zero power mismatches as the most difficult islanding case to be detected.

Table 2. Different scenarios for different power mismatch

	Total Power Demand		Power Mismatch	
	Active Power P (MW)	Reactive Power Q (MVAR)	Active Power P (MW)	Reactive Power Q (MVAR)
Scenario 1	14	7	5	2.641
Scenario 2	8	3.859	1	0.5
Scenario 3	9	4.359	0	0

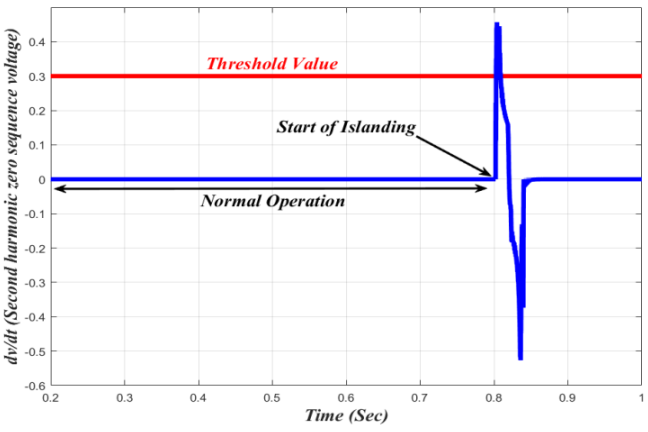

Fig. 5. $ROCO2Z$ variation for Scenario 1 (normal operation with large power mismatch versus islanding situation).

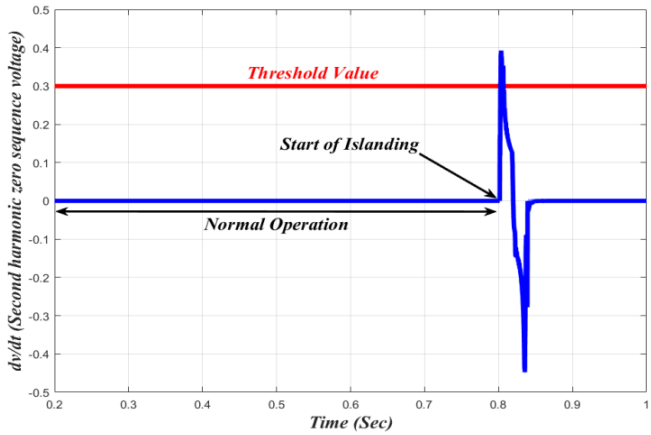

Fig. 6. *ROCO2Z* variation for Scenario 2 (normal operation with small power mismatch versus islanding situation).

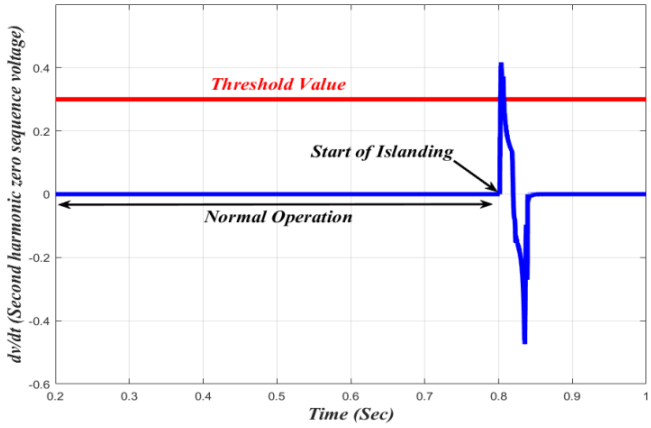

Fig. 7. *ROCO2Z* variation for Scenario 3 (normal operation with zero power mismatch versus islanding situation).

5.2. Performance of the proposed scheme during unbalanced loading conditions

Since the proposed technique depends on one of the symmetrical components, it is necessary to examine it during unbalanced loading conditions. Accordingly, the performance of ROCO2Z is also tested with an unbalanced load as shown in Fig. 8, where the islanding situation starts at 0.9 sec by opening the grid circuit breaker (CB5 in Fig. 4). In such case, phase A is loaded by 4 MW active power and 2 MVAR reactive power, phase B is loaded by 3 MW active power and 1.5 MVAR reactive power while phase C is loaded by 2 MW active power and 0.859 MVAR reactive power. Thus, the total three-phase load has still 9 MW active power and 4.359 MVAR reactive power conserving the zero power mismatch presented by Scenario 3 in Table 2.

As observed, *ROCO2Z* goes above the threshold value in less than half a cycle between 0.902 and 0.906 sec and thus the islanding case is successfully detected.

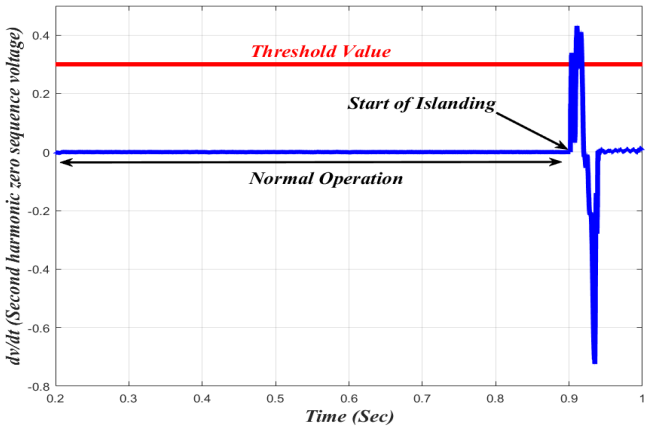

Fig. 8. Performance of the proposed scheme (*ROCO2Z* variation) for normal operation with unbalance load versus islanding situation.

5.3. Performance of the proposed scheme during normal switching events

The proposed *ROCO2Z* detector is also confirmed for normal switching. Load switching and capacitor switching are simulated, where the circuit breaker for load 2 of 4 MW & 2 MVAR (CB4) is closed at 0.5 sec and opened at 0.7 sec to simulate load variation, while the grid circuit breaker (CB5 in Fig. 4) is opened at 0.9 sec to create an islanding situation.

Fig. 9, illustrates the performance of the proposed technique during load variations versus islanding situation. As revealed, the increase of ROCO2Z for both events at load switching on and off was less than the setting threshold value. On the contrary, it has exceeded the threshold setting upon the occurrence of islanding.

A shunt capacitance of 1.41 MVAR is connected when the circuit breaker (CB1 in Fig. 4) is closed at 0.5 sec to evaluate the performance of the proposed technique against capacitor switching.

Fig. 10 shows that how the detector *ROCO2Z* exceeded the threshold value only after the grid circuit breaker (CB5 in Fig. 4) is opened at 0.8 sec when an islanding situation occurs, but it did not exceed the threshold value for capacitor switching event. Actually, when capacitor switching is commonly occurred for power factor correction, it causes a limited change in the voltage compared to the voltage variation in case of main grid outage (islanding condition).

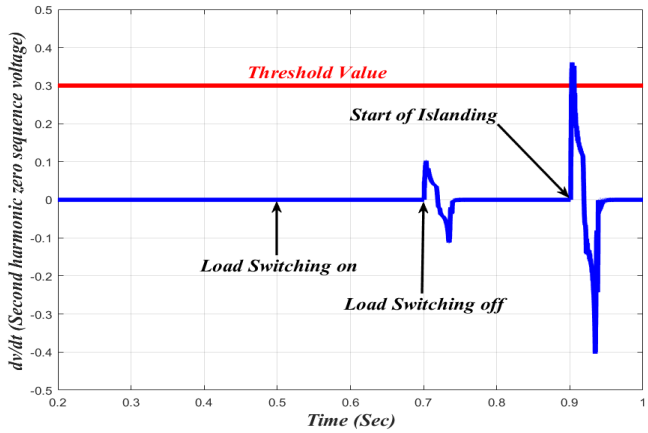

Fig. 9. Performance of the proposed scheme ($ROCO2Z$ variation) during load variations versus islanding situation.

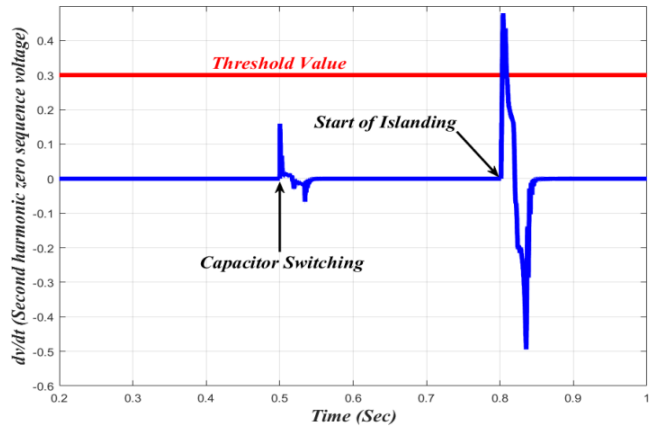

Fig. 10. Performance of the proposed scheme ($ROCO2Z$ variation) during capacitor switching versus the islanding situation.

5.4. Performance of the proposed scheme during power quality disturbances

The performance of the proposed detector based on $ROCO2Z$ for different power quality disturbances are also considered. For Fig. 11, the voltage sag is simulated by connecting part of loads where the circuit breaker (CB4 in Fig. 4) of load 2 which equals the fixed load 1 (9 MW & 4.359 MVAR) is closed at 0.6 sec. On the other hand, the voltage swell is simulated by disconnecting part of loads where the circuit breaker (CB4 in Fig. 4) of load 2 is opened at 0.6 sec, as shown in Fig. 12. For both tested cases, the grid circuit breaker (CB5 in Fig. 4) is opened at 0.8 sec to create an islanding situation.

As revealed from both Fig. 11, and Fig. 12, ROCO2Z has exceeded the setting only during the first cycle after the occurrence of islanding.

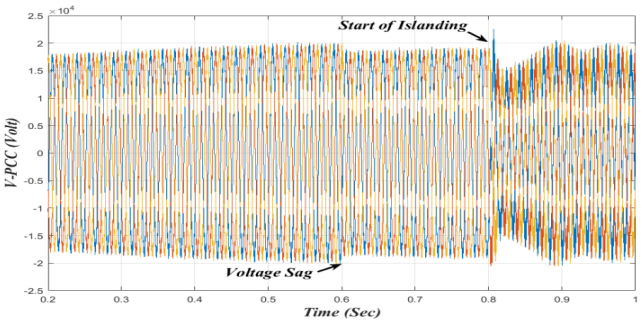

(a)

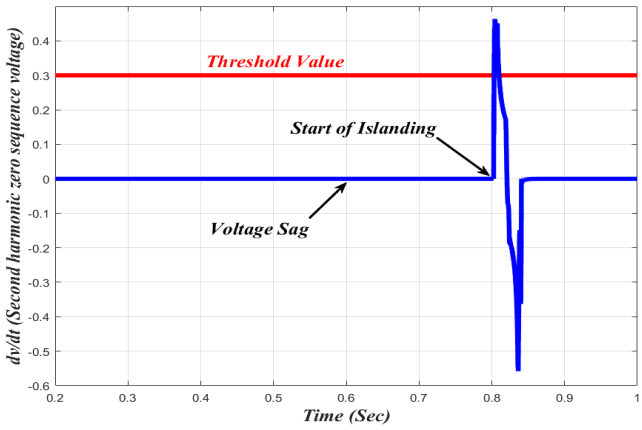

(b)

Fig. 11. (a) The three- phase voltage at PCC during voltage sag versus islanding situation, **(b)** Performance of the proposed scheme ($ROCO2Z$ variation)

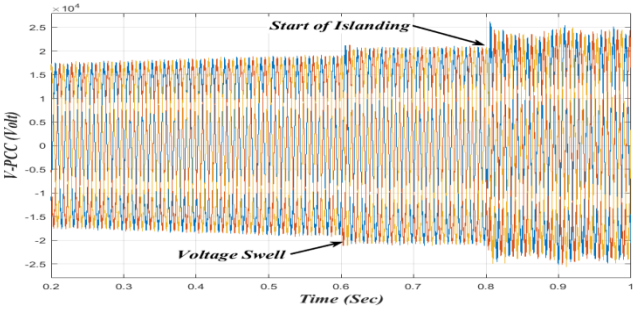

(a)

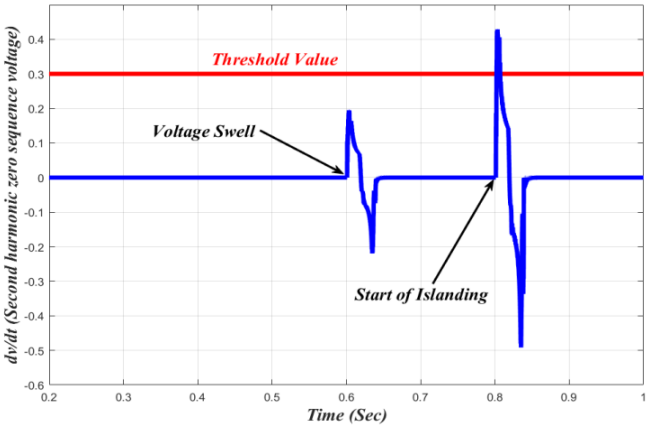

(b)

Fig. 12. (a) The three- phase voltage at PCC during voltage swell versus islanding situation. **(b)** Performance of the proposed scheme ($ROCO2Z$ variation).

5.5. Performance of the proposed scheme during faults

In this section, symmetrical and unsymmetrical faults are simulated at a zero power mismatch between the load demand and DG, to test the robustness of the proposed strategy.

A temporary three phase to ground fault at the end of transmission line 2 (F1 in Fig. 4) starts as a symmetrical fault at t=0.5 sec and then is cleared at t=0.6 sec without the operation of any circuit breaker. When the symmetrical fault occurs, significant changes in the voltage are detected by the proposed method. Nevertheless, $ROCO2Z$ can adequately distinguish this type of fault and islanding operation as shown in Fig. 13, where the grid circuit breaker (CB5 in Fig. 4) is opened at 0.9 sec to create an islanding situation.

An unsymmetrical fault presented in double line to ground has started at the end of transmission line 3 (F2 in Fig. 4) at t=0.4 sec and cleared at t=0.5 sec as shown in Fig. 14, without the operation of any circuit breaker. As shown, the proposed $ROCO2Z$ has effectively discriminated between islanding operation and this type of fault, where the grid circuit breaker (CB5 in Fig. 4) is opened at 0.8 sec for islanding operation. Besides, line to line and line to ground faults are also simulated and investigated in Fig. 15, and Fig. 16, respectively. The line to line fault occurs at F1 and starts at t=0.6 sec and then is cleared at t=0.7 sec without the operation of any circuit breaker, while the line to ground fault occurs t=0.5 sec at F2 and cleared at t=0.6 sec. While the islanding operation starts at 0.9 sec by opening the grid circuit breaker (CB5 in Fig. 4).

For all tested faults, as clearly shown, the proposed detector has accurately discriminated such faults against the event of islanding and avoided any maloperations.

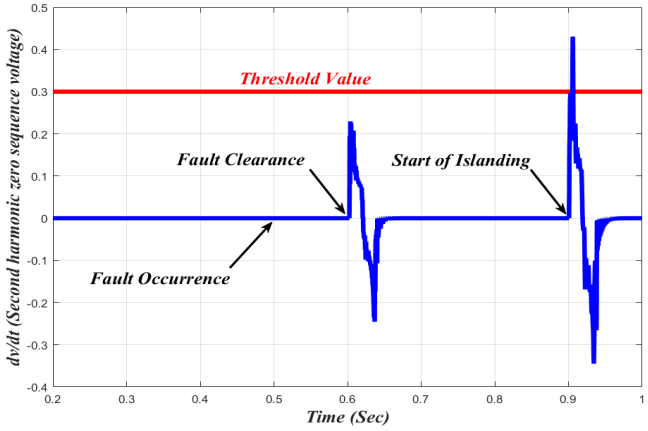

Fig. 13. Performance of the proposed scheme ($ROCO2Z$ variation) during three phase to ground fault versus islanding situation.

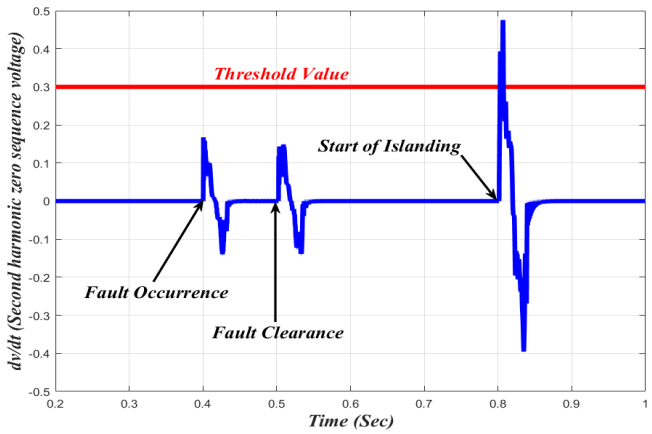

Fig. 14. Performance of the proposed scheme ($ROCO2Z$ variation) during double line to ground fault versus islanding situation.

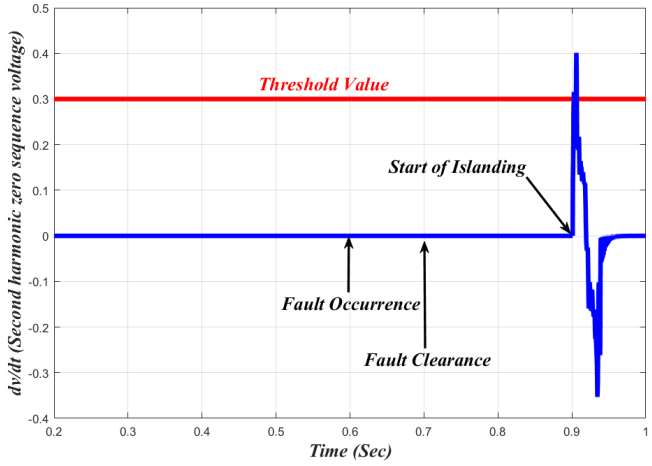

Fig. 15. Performance of the proposed scheme ($ROCO2Z$ variation) during line to line fault versus islanding situation.

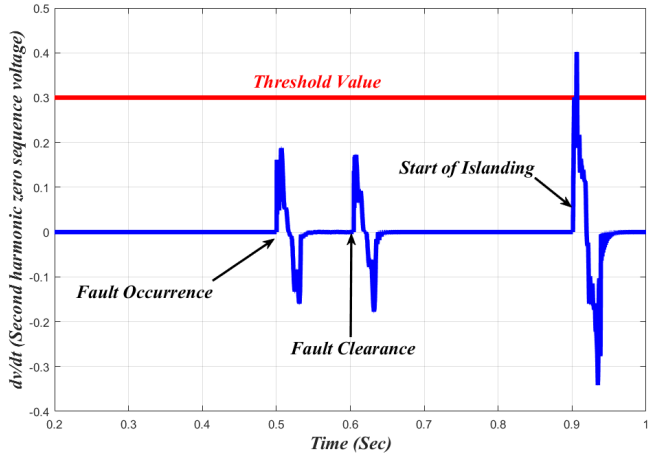

Fig. 16. Performance of the proposed scheme ($ROCO2Z$ variation) during line to ground fault versus islanding situation.

5.6. Performance of the proposed scheme during the one DGs outage

The proposed method not only can detect the islanding operation within the first cycle from the occurrence of islanding at the end of each DG in case of multi DGs in the

system (as shown in Fig. 4), but also it did not fail in islanding detection at the outage of one of the two DGs.

Thus, Fig. 17, shows the discrimination between the outage of the second DG and islanding situation, where the grid circuit breaker (CB5 in Fig. 4) is opened at 0.8 sec to create an islanding situation, and the second DG circuit breaker is opened at 0.5 sec (CB6 in Fig. 4).

Besides, Fig. 18, shows the difference between the outage of the main DG (CB3 in Fig. 4), which is opened at 0.6 sec and islanding situation where the grid circuit breaker (CB5 in Fig. 4) is opened at 0.9 sec.

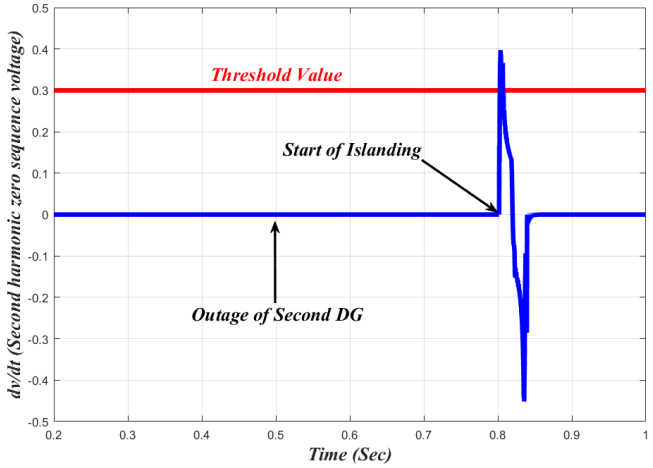

Fig. 17. Detection of islanding operation at the end of the main DG versus the second DG outage.

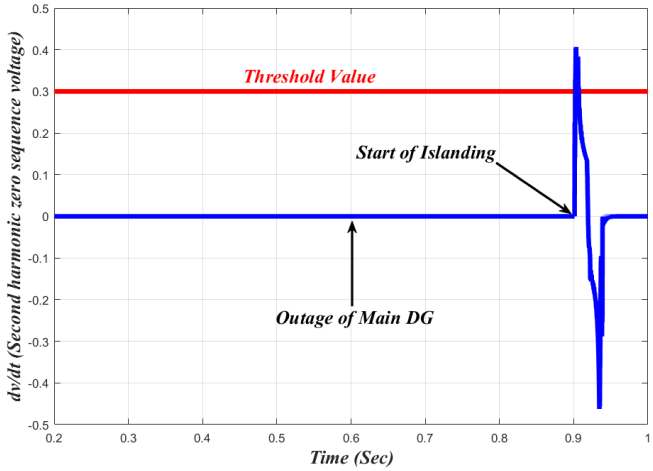

Fig. 18. Detection of islanding operation at the end of the second DG versus the main DG outage.

5.7. Discussion on the performance of the proposed scheme

Actually, and according to the achieved results of all carried out simulations to validate the performance of the proposed scheme either islanding cases or non-islanding cases, we can conclude that the proposed islanding detection technique has succeeded to detect the islanding operation in only one cycle without NDZ. It also avoids the false detection for other scenarios that have been compared versus islanding operation for the tested system. Table 3 summarizes the main achieved results of the proposed technique for all tested cases.

A simple comparison between the proposed technique and some published passive techniques based on harmonics is also carried out as illustrated in Table 4.

Table 3. Summary of the achieved results

Tested Scenarios			**Performance of Proposed Technique**
Islanding Cases	At Balanced Loading Conditions	Large Power Mismatch	Islanding is accurately detected - Within one cycle - Without NDZ
		Small Power Mismatch	
		Zero Power Mismatch	
	At Unbalanced Loading Conditions	Zero Power Mismatch	
Non Islanding Cases	Normal Switching Events	Load Switching	No false islanding event is detected
		Capacitor Switching	
	Power Quality Disturbances	Voltage Sag	
		Voltage Swell	
	Symmetrical & Unsymmetrical Faults	Three Phase to Ground Fault	
		Double Line to Ground Fault	
		Line to Line Fault	
		Line to Ground Fault	
	Outage of One of DGs	The Main DG Outage	
		The Second DG Outage	

6. Conclusion

Islanding detection using the rate of change of zero sequence of second harmonic voltage is proposed in this paper. The second harmonic order is selected as it is the clearest harmonic order in the tested system incorporating inverter-based DG of wind turbines with DFIG. In the proposed technique, the three phase voltage signals are measured at PCC in the distribution network then the DFT is applied to produce the signals of second harmonic voltage. Consequently, the rate of change of zero sequence component of the second harmonic voltage is computed and compared against a fixed setting as a threshold value to detect the islanding operation.

The effectiveness of the proposed method does not only appear through fast detection of islanding operation than some other methods without NDZ, but also it could differentiate effectively between the islanding case and other cases. It is clear from the achieved results of extensive simulations for several scenarios that the proposed technique could distinguish the islanding operation within only one cycle from the islanding occurrence without any NDZ. These scenarios have covered different cases such as

normal operation, load variation, unbalance loading, voltage sags and swells, capacitor switching, faults, and DG outage.

Finally, besides the developments have been accomplished in this paper, some possible future work may be considered such as applying the proposed method for a large distribution system includes large number of DG units and also modifying the proposed passive technique to a hybrid one to be suitable for systems of non-inverter based DG units.

Table 4. Comparison between the proposed technique and some published passive techniques based on harmonics

Method	Concept	NDZ	Detection time	Observations
Proposed technique	Rate of change of zero sequence of 2nd harmonic voltage	Non	1 cycle	It succeeded to differentiate between several scenarios
[21]	The 2nd harmonic voltage and current using ANN	Non for a preset power range	2 cycles	Its effectiveness is only confirmed for preset power range
[22]	Cumulative Reactive Power Harmonics	Non	2-5 cycles	Normal switching events are only tested versus islanding events
[23]	The 5th harmonic voltage variation	Non	2 sec	No much scenarios are tested
[24]	The harmonic variation of odd orders 3rd , 5th & 7th	Small	2 cycles	No much scenarios are tested
[25]	Under and Over voltage with THD	Small	Not revealed	Only different power mismatch scenarios are tested

References

[1] U. Sultan, A. Khairuddin, M. Aman, A. Mokhtar and N. Zareen. "A review of optimum DG placement based on minimization of power losses and voltage stability enhancement of distribution system". Renewable and Sustainable Energy Reviews, vol. 63, pp. 363-378, 2016 (Article).

[2] M. Bhaskar, S. Premalatha, A. Parameswaran, P. Dinesh and S. Dash."Protection of Stand-Alone Wind Energy Conversion System UsingBridge Type Fault Current Limiters". 8th International Conference on Renewable Energy Research and Applications (ICRERA), Brasov, Romania, pp. 892-897, 3-6 Nov. 2019 (Conference Paper).

[3] M. Hamidi and R. Chabanloo. " Optimal Allocation of Distributed Generation with Optimal Sizing of Fault Current Limiter to Reduce the Impact on Distribution Networks Using NSGA-I"I. IEEE Systems Journal, vol.13, pp. 1714 – 1724. 2019 (Article).

[4] F. Guarda, G. Cardoso, C. Silva and A. Morais. "Fault Current Limiter Placement to Reduce Recloser - Fuse Miss coordination in Electric Distribution Systems with Distributed Generation using Multi objective Particle Swarm Optimization". IEEE Latin America Transactions, vol. 16, no. 7, pp. 1914-1920. 2018 (Article).

[5] M. Maleki, R. Chabanloo and H. Javadi. "Method to resolve false tripping of non-directional over current relays in radial networks equipped with distributed generators". IET Generation, Transmission & Distribution, vol. 13, no. 4, pp. 485-494, 2019 (Article).

[6] Z. Abdmouleh, A. Gastli, L. Ben-Brahim, M. Haouari and N. Al-Emadi. "Review of Optimization Techniques Applied for the Integration of Distributed Generation from Renewable energy Sources". Renewable energy, vol. 113, pp. 266-280, 2017 (Article).

[7] A. Pouryekta, V. Ramachandaramurthy, N. Mithulananthan and A. Arulampalam." Islanding Detection and Enhancement of Microgrid Performance". IEEE Systems Journal, vol. 12, no. 4, pp. 3131-3141, 2018 (Article).

[8] S. Kermany, M. Joorabian, S. Deilami and M. Masoum. "Hybrid Islanding Detection in Microgrid with Multiple Connection Points to Smart Grids Using Fuzzy-Neural Network". IEEE Transactions on Power Systems, vol. 32, no. 4, pp. 2640-2651, 2017 (Article).

[9] G. Marchesan, M. Muraro, G. Cardoso, L. Mariotto and A. Morais. "Passive method for distributed-generation island detection based on oscillation frequency", IEEE Transactions on Power Delivery, vol. 31, no. 1, pp. 138-146, 2015 (Article).

[10] Y. Nie, H. Liang, W. Gu, M. Wu, J. Zhu and H. Liu. "A reliability evaluation method for distribution networks considering passive islanding detection failure". 5th International Conference on Renewable Energy Research and Applications (ICRERA), Birmingham, UK, pp. 678-683, 20-23 Nov. 2016 (Conference Paper).

[11] Y. Yoshida, K. Fujiwara, Y. Ishihara and H. Suzuki. "Performance verification of new active islanding detection methods for PV system by simulation". International Conference on Renewable Energy

Research and Applications (ICRERA), Nagasaki, Japan, 11-14 Nov. 2012 (Conference Paper).

[12] S. Liu, S. Zhuang, Q. Xu and J. Xiao. " Improved voltage shift islanding detection method for multi-inverter grid-connected photovoltaic systems", IET Generation, Transmission & Distribution, vol. 10, no. 13, pp. 3163-3169, 2016 (Article).

[13] M. Doumbia, M. Robitaille, K. Agbossou and R. Simard. "Islanding Detection Method for a Hybrid Renewable Energy System". International Journal of Renewable Energy Research (IJRER), Vol. 1, no. 1, pp. 41-53, 2011 (Article).

[14] K. Takeshita, O. Sakamoto, M. Maruyama and T. Harimoto. "Consideration on Voltage Fluctuation caused by Active Method of Islanding Detection of Photovoltaic Generation". 7th International Conference on Renewable Energy Research and Applications (ICRERA), Paris, France, pp. 606-611, 14-17 Oct. 2018 (Conference Paper).

[15] C. Li, C. Cao, Y. Cao, Y. Kuang, L. Zeng and B. Fang. "A review of islanding detection methods for microgrid", Renewable and Sustainable Energy Reviews, vol. 35, pp. 211-220, 2014 (Article).

[16] M. Khodaparastan, H. Vahedi. F. Khazaeli and H. Oraee. " A Novel Hybrid Islanding Detection Method for Inverter-Based DGs Using SFS and ROCOF". IEEE Transactions on Power Delivery. vol. 32, pp. 2162-2170, 2015 (Article).

[17] S. Manikonda and D. Gaonkar. "Comprehensive review of IDMs in DG system"s. IET Smart Grid, vol. 2, no. 1, pp. 11-24, 2018 (Article).

[18] A. Rostami, H. Abdi, M. Moradi, J. Olamaei and E. Naderi. "Islanding Detection based on ROCOV and ROCORP Parameters in the Presence of Synchronous DG Applying the Capacitor Connection Strategy". Electric Power Components and Systems, vol. 45, no. 3, pp. 315-330, 2017 (Article).

[19] K. Ahmad, J. Selvaraj and N. Abd Rahim "A review of the islanding detection methods in grid-connected PV inverters". Renewable and Sustainable Energy Reviews, vol. 21, pp. 756-766, 2013 (Article).

[20] B. Liu and K. Jia. "Impedance Estimation and the Total Harmonic Distortion Methods for Islanding Detection". 1st International Conference on Renewable Energy Research and Applications (ICRERA), Nagasaki, Japan, 11-14 Nov. 2012 (Conference Paper).

[21] A. Abd-Elkader, D. Allam and E. Tageldin. " Islanding detection method for DFIG wind turbines using artificial neural networks", Electrical Power and Energy Systems, vol.62, pp. 335-343, 2014 (Article).

[22] R. Haider, T. Ghanbari and C. Kim. " Islanding Detection Scheme for Inverter-Based Distributed Generation Systems Using Cumulative Reactive Power Harmonics". Journal of Electrical Engineering & Technology, vol. 14, pp. 1907-1917, 2019 (Article).

[23] J. Merino, P. Araya, G. Venkataramanan and M. Baysal. "Islanding Detection in Microgrids Using Harmonic Signatures". IEEE Transactions on Power Delivery, vol. 30, no. 5, pp. 2102-2109, 2015 (Article).

[24] R. Haider, C. Kim, T. Ghanbari and S. Bukhari. "Harmonic-signature-based islanding detection in grid-connected distributed generation systems using Kalman filter". IET Renewable Power Generation, vol. 12, no. 15, pp. 1813-1822, 2018 (Article).

[25] R. Somalwar, S. Kadwane and D. Mohanta. "Harmonics-Based Enhanced Passive Islanding Method for Grid-Connected System". Electric Power Components and Systems, vol. 45, no. 14, pp 1554-1563, 2017 (Article).

[26] C. Papadimitriou, V. Kleftakis and N. Hatziargyriou. "Control strategy for seamless transition from islanded to interconnected operation mode of microgrids". Journal of Modern Power Systems and Clean Energy, vol. 5, pp. 169-176, 2017 (Article).

[27] K. Yang. "Wind-Turbine Harmonic Emissions and Propagation through a Wind Farm". Sweden, Luleå University of Technology, Department of Engineering Sciences and Mathematics. 2012 (Thesis).

[28] M. Bollen and K. Yang. " Harmonic aspects of wind power integration". Journal of Modern Power Systems and Clean Energy, vol. 1, pp. 14-21, 2013 (Article).